



Geophysical Research Letters®

RESEARCH LETTER

10.1029/2023GL105552

Key Points:

- We document the rapid thaw and subsidence of saline permafrost below a shallow thermokarst lake in Arctic Alaska
- We hypothesize that rapid saline permafrost degradation is occurring below shallow arctic lakes at sub-zero temperatures
- Thawing saline permafrost may be contributing to an increase in landscape change rates in the Arctic

Correspondence to:

B. M. Jones,
bmjones3@alaska.edu

Citation:

Jones, B. M., Kanevskiy, M. Z., Parsekian, A. D., Bergstedt, H., Ward Jones, M. K., Rangel, R. C., et al. (2023). Rapid saline permafrost thaw below a shallow thermokarst lake in Arctic Alaska. *Geophysical Research Letters*, 50, e2023GL105552. <https://doi.org/10.1029/2023GL105552>

Received 18 JUL 2023

Accepted 1 NOV 2023

Author Contributions:

Conceptualization: Benjamin M. Jones, Mikhail Z. Kanevskiy, Andrew D. Parsekian, Helena Bergstedt, Melissa K. Ward Jones, Yuri Shur

Formal analysis: Benjamin M. Jones, Mikhail Z. Kanevskiy, Andrew D. Parsekian, Helena Bergstedt, Melissa K. Ward Jones, Rodrigo C. Rangel

Investigation: Benjamin M. Jones, Mikhail Z. Kanevskiy, Andrew D. Parsekian, Helena Bergstedt, Melissa K. Ward Jones, Rodrigo C. Rangel

Methodology: Benjamin M. Jones, Mikhail Z. Kanevskiy, Andrew D. Parsekian, Helena Bergstedt, Melissa K. Ward Jones, Rodrigo C. Rangel

Visualization: Benjamin M. Jones, Andrew D. Parsekian, Helena Bergstedt

© 2023. The Authors.

This is an open access article under the terms of the [Creative Commons Attribution-NonCommercial-NoDerivs License](#), which permits use and distribution in any medium, provided the original work is properly cited, the use is non-commercial and no modifications or adaptations are made.

Rapid Saline Permafrost Thaw Below a Shallow Thermokarst Lake in Arctic Alaska

Benjamin M. Jones¹ , Mikhail Z. Kanevskiy¹ , Andrew D. Parsekian^{2,3} , Helena Bergstedt⁴, Melissa K. Ward Jones¹, Rodrigo C. Rangel² , Kenneth M. Hinkel⁵, and Yuri Shur¹

¹Institute of Northern Engineering, University of Alaska Fairbanks, Fairbanks, AK, USA, ²Department of Geology & Geophysics, University of Wyoming, Laramie, WY, USA, ³Department of Civil & Architectural Engineering & Construction Management, University of Wyoming, Laramie, WY, USA, ⁴b.geos, Korneuburg, Austria, ⁵Michigan Technological University, Houghton, MI, USA

Abstract Permafrost warming and degradation is well documented across the Arctic. However, observation- and model-based studies typically consider thaw to occur at 0°C, neglecting the widespread occurrence of saline permafrost in coastal plain regions. In this study, we document rapid saline permafrost thaw below a shallow arctic lake. Over the 15-year period, the lakebed subsided by 0.6 m as ice-rich, saline permafrost thawed. Repeat transient electromagnetic measurements show that near-surface bulk sediment electrical conductivity increased by 198% between 2016 and 2022. Analysis of wintertime Synthetic Aperture Radar satellite imagery indicates a transition from a bedfast to a floating ice lake with brackish water due to saline permafrost thaw. The regime shift likely contributed to the 65% increase in thermokarst lake lateral expansion rates. Our results indicate that thawing saline permafrost may be contributing to an increase in landscape change rates in the Arctic faster than anticipated.

Plain Language Summary In this study, we combine direct field measurements, near-surface geophysical studies, and remote sensing change detection to document the rapid thaw of saline permafrost below a shallow thermokarst lake on the Arctic Coastal Plain of northern Alaska. Thaw of ice-rich saline permafrost resulted in an increase in the lake depth by 0.6 m over a 15-year period. The transition from a bedfast ice lake to a floating ice lake with brackish water is responsible for the increase near-surface bulk sediment electrical conductivity and likely contributed to an increase in the lateral expansion rate of the lake. Our findings indicate that active permafrost thaw is likely occurring below shallow arctic lakes at temperatures below 0°C.

1. Introduction

The formation and drainage of lakes have shaped lake and drained lake basin (L-DLB) landscapes in lowland permafrost regions (Grosse et al., 2013; Jones et al., 2022). The long-term evolution of L-DLB landscapes is well documented (Jorgenson & Shur, 2007; Wolfe et al., 2020); however, few studies have directly observed L-DLB surface dynamics in the field using observational data sets (e.g., Arp et al., 2023; Jones & Arp, 2015; Jones et al., 2023b; Lantz et al., 2022). Even fewer studies have observed sub-surface dynamics associated with sub-lake permafrost thaw and talik formation (e.g., Creighton et al., 2018; Roy-Leveillee & Burn, 2017). Further to our knowledge, no studies have considered the impact of warming saline permafrost on rapid thaw below shallow thermokarst lakes.

Warming of permafrost is well documented on the Arctic Coastal Plain (ACP) of northern Alaska (Biskaborn et al., 2019). Nevertheless, the ACP region is typically considered to be relatively safe from thaw since permafrost temperature remains below 0°C. However, in saline permafrost, the thawing point of the pore ice is depressed such that permafrost can thaw at sub-zero temperatures (Nersesova & Poire, 1952; Wan et al., 2015). Considering high ground-ice content in saline soils of the upper permafrost on the ACP (Kanevskiy et al., 2013), we may expect significant thaw settlement as a result of permafrost warming at temperatures below 0°C. Further, this thaw settlement may occur earlier below shallow thermokarst lakes, given the elevated mean annual permafrost temperature below lakes compared to terrestrial environments (Arp et al., 2016).

Saline permafrost is widely distributed in the continuous permafrost zone in the Northern Hemisphere (Bouchkov, 2002, 2003). Saline permafrost is estimated to underly ~35% of the continuous permafrost region

Writing – original draft: Benjamin M. Jones, Mikhail Z. Kanevskiy, Andrew D. Parsekian, Helena Bergstedt, Melissa K. Ward Jones, Rodrigo C. Rangel, Kenneth M. Hinkel, Yuri Shur

(Figure 1a; Brouchkov, 2003). The origin of the salinity in this region is primarily thought to result from accumulation of marine sediment during periods in the Late Quaternary when sea level was higher than today (Brigham-Grette & Hopkins, 1995; Brouchkov, 2003). Near-surface saline permafrost may be encountered at depths up to 50 m below the ground surface (bgs) (Gilichinsky et al., 2003; Hivon & Sego, 1993) and in some areas it occurs in the upper several meters (Bristol et al., 2021; Brown, 1969; Dafflon et al., 2016; Iwahana et al., 2021).

The influence of saline permafrost on infrastructure stability in the Arctic has been considered (e.g., Biggar & Sego, 1993; Miller & Johnson, 1990), and the freeze/thaw behavior of saline permafrost has been studied in the laboratory (e.g., Wan et al., 2015). However, only limited attention has been given to the way in which natural processes in the Arctic are influenced by the occurrence and thaw of saline permafrost. Saline permafrost thaw is thought to be a factor in increasing erosion rates along Arctic coastlines (Bristol et al., 2021; Jones et al., 2018; Lorenson et al., 2018). In addition, near-surface geophysical studies on the ACP focused on quantifying permafrost degradation below lakes (Creighton et al., 2018; Parsekian et al., 2019) as well as permafrost aggradation in drained lake basins (Rangel et al., 2021) has revealed the likely influence of salinity on the presence of unfrozen liquid pore water in the permafrost.

In this study, we document the rapid thaw of saline permafrost below a shallow thermokarst lake on the ACP of northern Alaska. We conducted repeat drilling-based surveys at East Twin Lake near Utqiagvik, Alaska between 2008 and 2023 (Figures 1b and 1c). These field data were integrated with transient electromagnetic (TEM) near-surface geophysics soundings in 2016 and 2022 and analysis of a time-series of wintertime Synthetic Aperture Radar (SAR) satellite imagery from 2015 to 2022 to assess changes in lake and sub-lake properties. Finally, we assessed the impact of thawing saline permafrost on shore erosion of East Twin Lake with remotely sensed imagery available between 1948 and 2022. Our findings indicate that active permafrost thaw is occurring below shallow thermokarst lakes underlain by saline permafrost and that thawing saline permafrost may be contributing to an increase in landscape change rates in the Arctic.

2. Study Area

The ACP of northern Alaska is located in the continuous permafrost zone with mean annual ground temperatures at the depth of zero annual amplitude averaging -4 to -8°C (Biskaborn et al., 2019). The presence of saline permafrost on the Younger Outer Coastal Plain (YOCP) and Outer Coastal Plain (OCP) of the ACP was first described in the 1960s (Brown, 1969; O'Sullivan, 1966). This region is also known to contain numerous lakes of various origin (i.e., thermokarst vs. non-thermokarst) (Jones et al., 2022; Jorgenson & Shur, 2007). Lake depth relative to maximum wintertime ice thickness is a key characteristic that controls thermokarst lake expansion and talik development (Arp et al., 2011, 2012). Based on Grunblatt and Atwood (2014), $>80\%$ of the lakes on the YOCP and OCP regions are thought to typically freeze to their bed each winter (Figure 1b). One such historically bedfast ice lake is the 130 ha East Twin Lake located near Utqiagvik, AK (Figure 1c). It is situated near the coast of Elson Lagoon, but it is not subject to storm surges given its height (2.8 m) above sea level.

3. Methods

During April 2008, we drilled four holes through the ice on East Twin Lake, a bedfast ice lake at the time, along an east to west transect across the middle of the lake to measure ice thickness and lake depth (Figure 1c). We also drilled three holes in West Twin Lake, an adjacent floating ice lake (Figure 1c). During May 2023, we redrilled at the same seven locations and added an additional eight locations in East Twin Lake. In addition to measuring ice thickness and lake depth in 2023, we measured lake water specific electrical conductivity (EC) below the ice, the thickness of sub-lake thawed sediment, and thawed sediment temperatures. In April 2022, we collected a tundra permafrost core in the center of an ice-wedge polygon adjacent to the lake to take measurements on ground-ice content and specific EC. In May 2023, we collected a near-shore, sub-lake permafrost core. The ice content of the soil was determined in the laboratory from an initial weight of soil in a frozen state and after oven-drying (90°C , 72 hr). Gravimetric (GMC) and volumetric moisture contents (VMC), and excess-ice contents (EIC) were determined according to Shur et al. (2021). Specific EC of the pore fluids was measured in thawed samples with a handheld sonde before drying.

In May 2016 and April 2022, we conducted transient electromagnetic (TEM) geophysical soundings using an ABEM WalkTEM instrument (GuidelineGeo, Stockholm, SE) at East Twin Lake (Parsekian et al., 2018). The

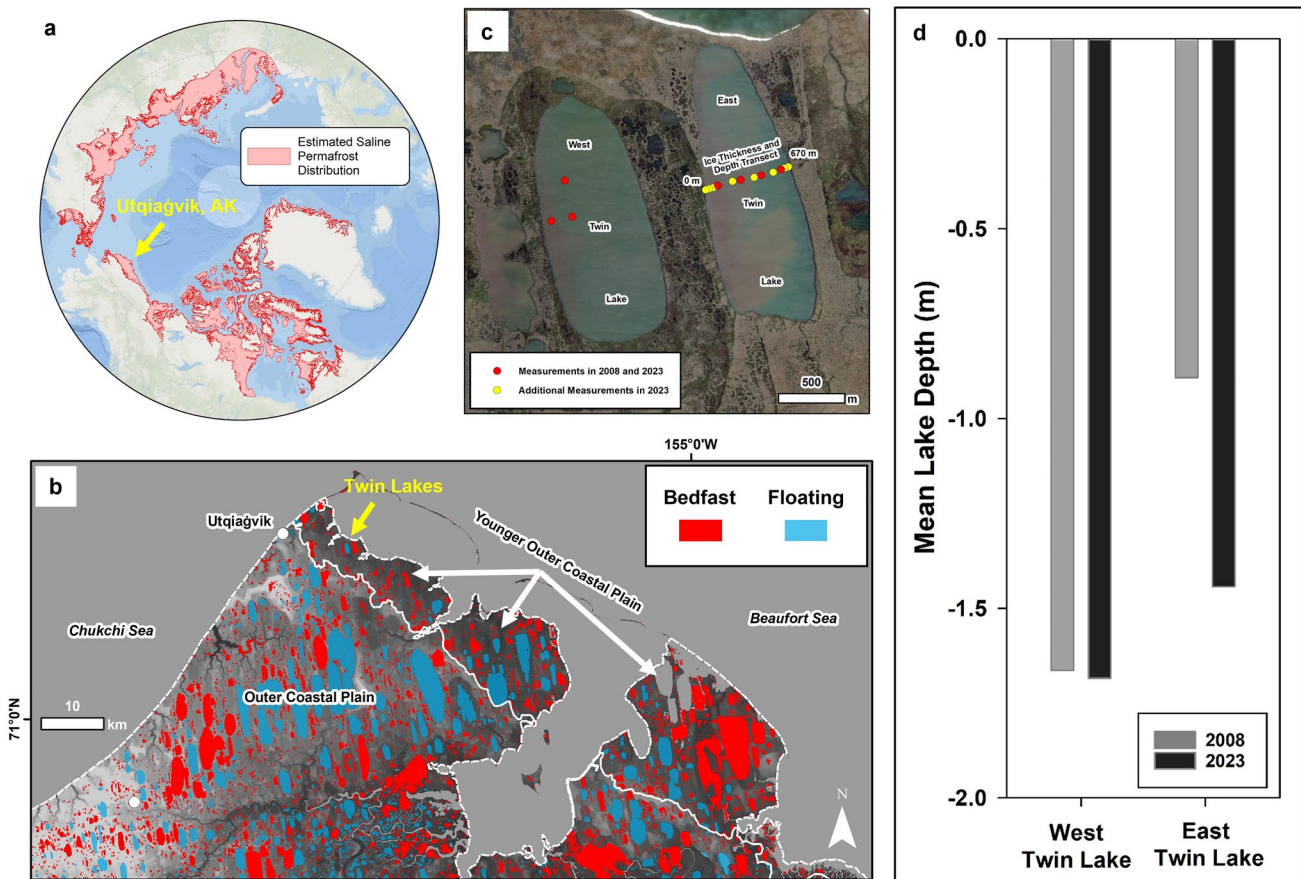


Figure 1. The study site location in the context of saline permafrost distribution in the Arctic. (a) Estimated occurrence of saline permafrost in the northern circumpolar permafrost region (from Brouckov, 2003). (b) Shallow thermokarst lakes that typically freeze to their bed are prevalent on the Younger Outer Coastal Plain (YOCOP) and OCP regions on the ACP of northern Alaska (Grunblatt & Atwood, 2014). In the area shown in (b), 86% of the lakes and 49% of the lake area is classified as bedfast. (c) The location of drill holes in 2008 and 2023 in East and West Twin Lakes (imagery copyright MAXAR). (d) The mean lake depth measured at East Twin ($n = 4$) and West Twin ($n = 3$) Lakes in 2008 and 2023.

instrument configuration consisted of a 1,600 m² transmitter loop and 200 and 5 m² receiver loops, with all loops centered around a common point on the ice near the center of the lake. Measurement frequencies of 240 Hz (28-time gates) and 30 Hz (38-time gates) were used and both were recorded on each receiver loop. The data were processed using AarhusInv SPIA (Aarhus GeoSoftware, Aarhus, DE). First, data were inspected for noise in early and late times, and consistency between receiver coils; points that could not be visually distinguished from the noise floor were manually rejected. Finally, a smooth 1D inversion with 20 model layers was performed. We then followed an adaptation of Archie's (1942) equation (Daniels et al., 1976; Hauck, 2002; Hauck & Mühll, 2003) to calculate the change in pore ice based on the measured average bulk EC values from TEM, local estimates of porosity (0.45 m³ m⁻³; Hinkel et al., 2001), and the measured pore water specific EC.

We utilized SAR satellite imagery from Sentinel-1 to create a time-series of backscatter values for three thermokarst lakes on the ACP of northern Alaska. Analysis of SAR satellite imagery is commonly used to distinguish between bedfast and floating ice lakes due to the ability of the sensor to detect differences in the dielectric properties associated with lake ice in contact with frozen sediments versus lake ice in contact with liquid water (Engram et al., 2018; Murfitt & Duguay, 2021; Weeks et al., 1978). The three lakes were selected based on their lake ice regime behavior over the period of record from 2015 to 2022. Sentinel-1 data was processed using the Alaska Satellite Facility (ASF) on demand capabilities for radiometric terrain correction. A time series for the center of the selected lakes were extracted and an incidence angle correction to 40° was applied following the approach by Widhalm et al. (2018) and Pointner et al. (2019). More than 250 Sentinel-1 acquisitions were selected, spanning the years 2015–2022, focusing on the period of maximum winter ice growth on the ACP (March to April).

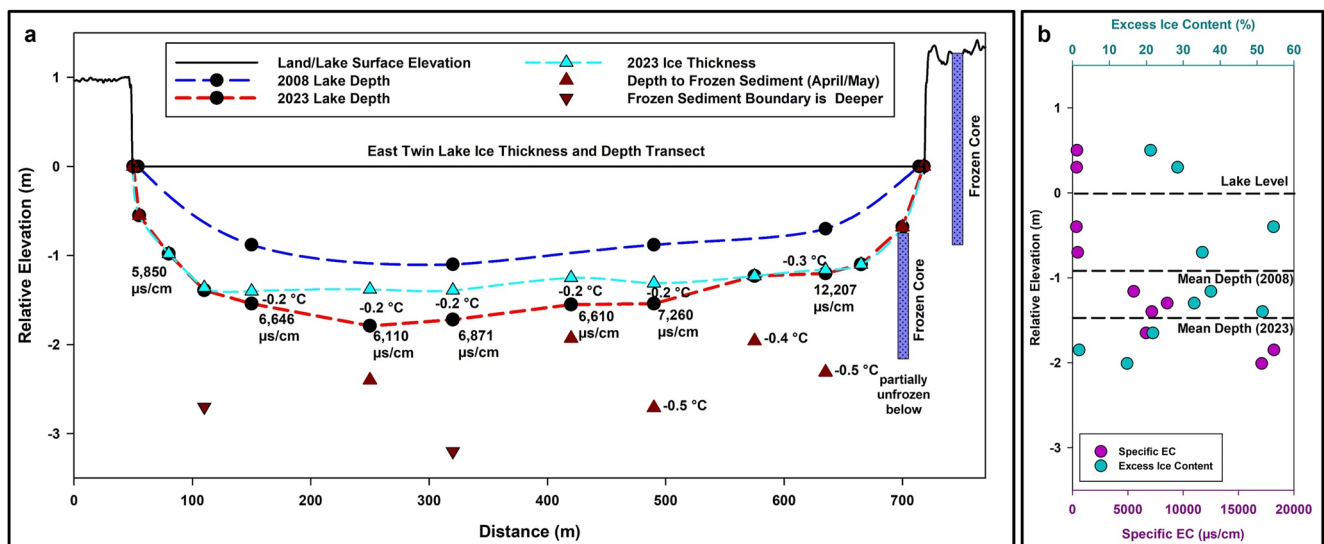


Figure 2. The evolution of East Twin Lake between 2008 and 2023. (a) In 2008, East Twin Lake was frozen to its bed with a mean depth of 0.9 m. In early May 2023, the same four locations were ~ 0.6 m deeper. In May 2023, we also measured additional lake depths, temperature and specific EC of water below the lake ice, and thawed lake sediments at sub-zero temperatures. (b) Specific EC and EIC values obtained from the two frozen cores (a). Saline permafrost sediments were encountered ~ 1 m below the lake surface, and their specific EC increased from 5,500 $\mu\text{S}/\text{cm}$ to $>18,000$ $\mu\text{S}/\text{cm}$ at a depth of 1.8 m below the lake surface. Excess ice content of saline permafrost was as high as 20%–50%.

We reconstructed the lateral expansion rate of East Twin Lake using historical aerial photography, commercial high-resolution satellite imagery, and the USGS Digital Shoreline Analysis System (DSAS) tool (Himmelstoss et al., 2021). Imagery was available for 1948, 1979, 2002, and 2022. Thermokarst lake expansion rates were measured every 3 m around the lake perimeter and the results were reported as the net expansion per unit time in each of the three time periods.

4. Results

Between 2008 and 2023, the measured depth of East Twin Lake increased from 0.89 to 1.44 m, or a 62% increase, based on late-winter point measurements from the frozen lake surface (Figure 1d). Whereas, at West Twin Lake, the depth remained approximately the same (1.66 m in 2008 and 1.68 m in 2023) indicating that lake levels were similar in the two years. Further, in East Twin Lake we measured a lowering of the frozen ground table relative to the lake surface by 1.61 m, 1.85 m, and more than 2.11 m over the 15-year period (Figure 2a). The additional eight measurement locations in 2023 allowed us to better resolve the bathymetry of the lake, late winter ice thickness, lake water specific EC, thickness of unfrozen sediments, and lakebed sediment temperatures (Figure 2a). Thawed lakebed sediment temperatures above the frozen ground table ranged from -0.4 to -0.6°C , which we relate to high salinity of thawing sediments.

The specific EC values of the permafrost obtained from two permafrost cores—adjacent to and below East Twin Lake—increase with depth (Figure 2b). Samples from 0.5 m above and 1 m below the surface of the lake, as measured adjacent to the lake, averaged 401 $\mu\text{S}/\text{cm}$. However, from 1.0 to 1.7 m below the surface of the lake the specific EC of the permafrost increases to an average of 6,980 $\mu\text{S}/\text{cm}$. Below 1.7 m the specific EC of the saline permafrost increases further to 17,100 $\mu\text{S}/\text{cm}$ at 2.1 m below the lake surface. EIC in the upper permafrost varied from 20% to 55% from ~ 0.3 m above and 1.7 m below the lake surface; it significantly decreased below 1.7 m and varied from 0.5% to 15% at 1.8–2.2 m below the lake surface (Figure 2b). The elevated values of EIC correspond approximately to the measured increase in the lake depth due to subsidence that has been caused by thaw of ice-rich saline permafrost.

The TEM geophysical soundings at East Twin Lake (Figure 3) revealed a general trend of increasing bulk EC from the surface to a depth of 10 m, then decreasing bulk EC below that depth. We interpret the high bulk EC around 10 m depth to be associated with high salinity in sediments or a brine layer. There is one ground-truth probe point at ~ 320 m (Figure 2) indicating that the frozen boundary is deeper than 3.25 m which

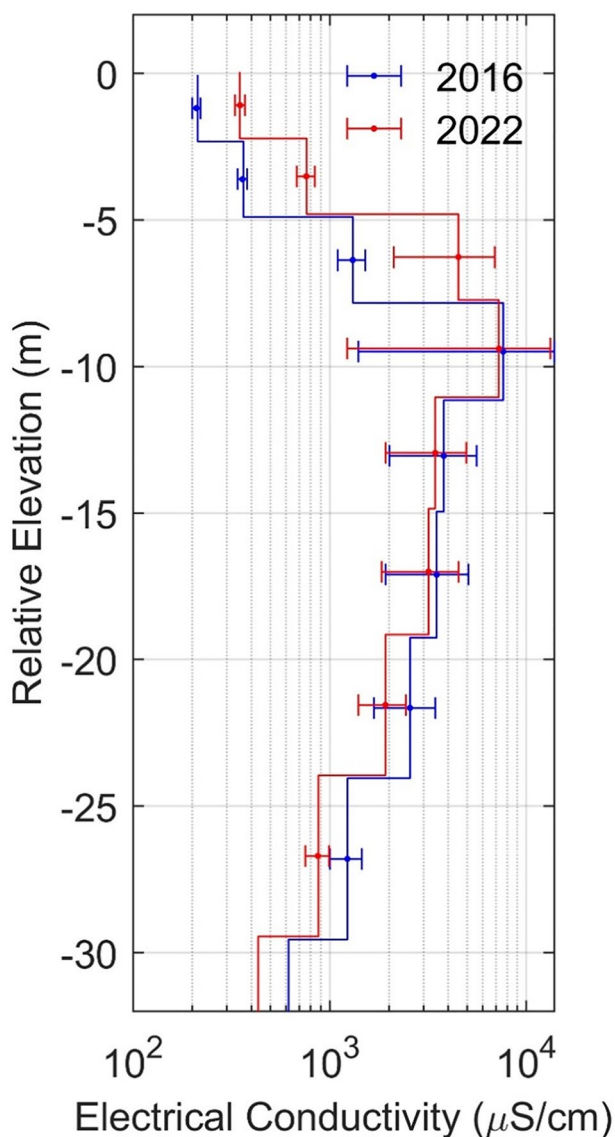


Figure 3. TEM measurements from the middle of East Twin Lake in 2016 and 2022. The increase in bulk EC between 0 and 8 m is likely in response to saline permafrost thaw.

lake expansion rates. The rapid acceleration in lake expansion rates observed at East Twin Lake likely makes it more vulnerable to drainage in the future (Jones et al., 2020).

Our TEM geophysical soundings provide the first known measurement of changing bulk EC associated with permafrost degradation below a thermokarst lake. Previous similar examples of ice content loss have been observed on subaerial terrestrial permafrost (Hauck, 2002; Hauck & Mühll, 2003). The change in ice content calculation based on time-lapse TEM measurements of sub-lake resistivity is enabled because we can assume the sub-lake environment remains saturated with brine (Parsekian et al., 2019). Assuming that the water resistivity and mineral phase remain constant, then reduction of ice in pore spaces would be the only property to explain the difference in resistivity over time. Differences in in situ measured pore water electrical properties (Figure 2) and bulk electrical conductivity measured by TEM (Figure 3) in this study are expected due to differences in sampling volumes of the two measurements and the fact that the sonde measures fluid electrical conductivity while the TEM measures bulk electrical properties (Rangel et al., 2021).

is consistent with the TEM measurements at this location. The mean bulk EC of near-surface permafrost up to 8 m below the lake surface increased by 198% between 2016 and 2022. Following the petrophysical calculation of pore ice reduction presented in Hilbich et al. (2008) and Hauck (2002), we estimate that the fraction of the pore space occupied by ice (Figure 2b), ΔS_i (i.e., interpreted as ice loss), is -0.2 for the lower pore water specific EC range ($S_i, 2016 = 0.4$; $S_i, 2022 = 0.2$) and -0.1 for the higher pore water specific EC range ($S_i, 2016 = 0.6$; $S_i, 2022 = 0.5$). These results provide an additional line of evidence highlighting that change between 2016 and 2022 is not solely limited to an increase in lake depth, but rather the effects extend to ~ 8 m below the surface.

We measured a decrease in the SAR backscatter for East Twin Lake between 2018 and 2019 (Figure 4). The backscatter values decreased from a typical bedfast ice lake to one that is known to have floating ice with brackish water underlying the ice (Lake 113). In contrast, West Twin Lake consistently displayed the highest backscatter values associated with floating ice overlying relatively fresh water compared to the other study sites (Figure 4).

East Twin Lake expanded laterally at a mean annual rate of 0.26 m/yr between 1948 and 1979. The mean lake expansion rate of the entire lake perimeter remained consistent (0.26 m/yr) between 1979 and 2002. However, between 2002 and 2022 it increased to 0.43 m/yr (Figure 5), with more than 70% of the measurement sites around the perimeter of the lake exceeding the historical average. Maximum lake expansion rates also increased from a historical value of 0.9–1.3 m/yr (Figure 5).

5. Discussion

Our results from East Twin Lake indicate that thaw susceptible saline permafrost is located below shallow thermokarst lakes. East Twin Lake transitioned from a bedfast to floating ice lake despite its depth being much shallower than the maximum annual winter time lake ice thicknesses in the Utqiagvik region that averaged 140 cm from 2008 to 2019 (Arp & Cherry, 2020). This should have retained sub-zero permafrost temperatures below the 0.9 m lake depth that was initially measured in 2008 (Arp et al., 2012). However, thawing of ice-rich saline permafrost has occurred due to increase in soil temperatures (which were likely still negative) and resulted in thaw subsidence and an increase in lake depth. The depth of East Twin Lake is approaching that of the adjacent West Twin Lake that had already transitioned to a floating ice lake at some point in the past. The transition of East Twin Lake from a bedfast ice lake to a floating ice lake has likely contributed to the 65% increase in

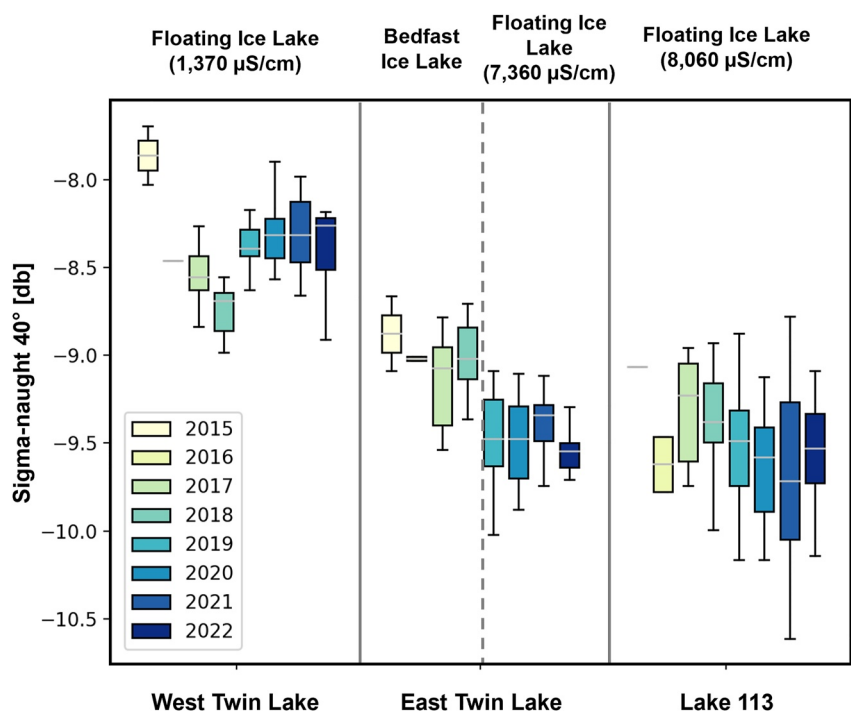


Figure 4. Late winter Sentinel-1 backscatter plots (2015–2022) for a floating ice lake with relatively freshwater (West Twin Lake), a lake that transitioned from bedfast to floating with brackish water below the ice (East Twin Lake), and a floating ice lake with brackish water below the ice over the entire study period (Lake 113). Under-ice lake water specific EC values are shown in parentheses.

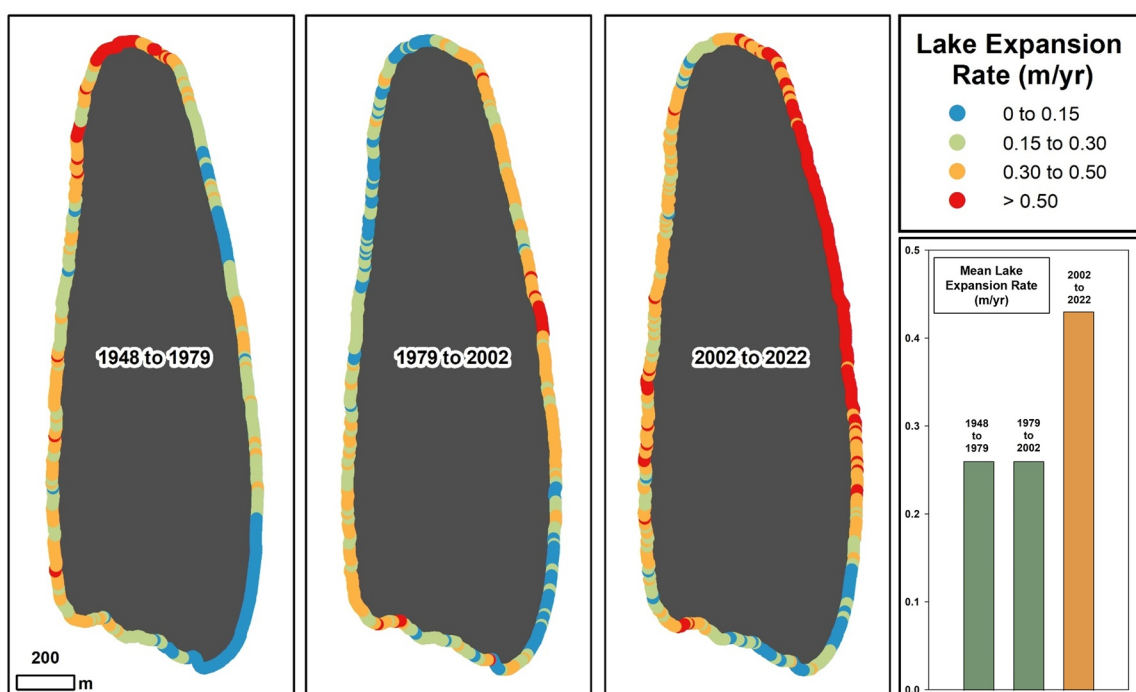


Figure 5. Remote sensing change detection analysis for East Twin Lake between 1948 and 2022. The regime shift from a grounded-ice to a floating-ice lake likely resulted in a 65% increase in lateral lake expansion rates.

Our study also demonstrates the ability to detect sub-lake, saline permafrost degradation using SAR imagery which could allow for identification of this process across L-DLB regions in the Arctic. Low backscatter values for areas of ice overlaying brackish water is a well-known phenomenon in the field of sea ice studies (Dammann et al., 2018). However, our results indicate there is a novel signature apparent in the VH polarization that can distinguish between floating ice lakes with freshwater versus brackish water underlying the ice. Results from the analysis suggest that SAR-based approaches may underestimate sub-lake permafrost thaw since floating ice lakes with brackish water have previously been classified as being bedfast (Figure 1; Engram et al., 2018).

Permafrost-region landscape change rates are increasing around the circum-Arctic; however, the role of warming saline permafrost on landscape change rates remains largely unstudied at this point. Overlaying a circumpolar map of lakes from Bartsch et al. (2017) with the estimated occurrence of saline permafrost distribution from Brouchkov (2003) shows the presence of more than 1 million lakes larger than 2.5 ha. Bartsch et al. (2017) indicated that 12% of the lake area in the saline permafrost region was mapped as bedfast ice. Furthermore, their data shows a tendency for smaller lakes to be almost entirely bedfast. Considering the prevalence of numerous smaller lakes in the Arctic (Muster et al., 2019), the true bedfast lake ice area in saline permafrost regions is substantially higher than these estimates. Bartsch et al. (2017) also found that the proportion of bedfast lake ice was higher in permafrost regions with high soil organic carbon contents. The connection between shallow lakes, thawing saline permafrost, and the potential to alter hydrologic processes and mobilize organic carbon previously stored in permafrost is an important topic for future study.

6. Conclusion

In this study, we document the rapid thaw of saline permafrost below a large, shallow thermokarst lake near Utqiāġvik, Alaska. The thaw of warming, ice-rich saline permafrost has occurred while soil temperatures were likely still below 0°C, resulting in thaw subsidence that increased the lake depth by 0.6 m over a 15-year period. The transition from a bedfast ice lake to a floating ice lake with brackish water was detected in direct field measurements, near-surface geophysical studies, and satellite-based SAR imagery. The lake ice regime shift likely contributed to a 65% increase in thermokarst lake expansion rates since 2002. We found that rapid saline permafrost thaw is occurring below a shallow arctic lake that historically froze to its lakebed in the winter. We expect that thawing saline permafrost will contribute to an increase in landscape change rates in the Arctic.

Data Availability Statement

The data that support the findings of this study are available at the NSF-funded Arctic Data Center. Measurements on lake depth, ice thickness, specific electrical conductivity of unfrozen lake water and thawed permafrost soils, thawed sediment temperature, depth to frozen ground, excess ice content, Sentinel-1 SAR backscatter time series values from 2015 to 2022, lateral thermokarst lake expansion rates from 1948 to 2020, and the near-surface geophysical TEM data from 2022 are available from Jones et al. (2023a). The near-surface geophysical TEM data collected in 2016 are available from Parsekian et al. (2018).

Acknowledgments

This research was supported by the National Science Foundation (OPP-1806213, 1806202, 1806287, 1820883). This work was further supported by the European Research Council project number 951288. We thank UIC Science, Battelle ARO, and the NSF RSL program for facilitating our field research efforts. We thank A.L. Creighton and N. Ohara for their assistance during geophysical data acquisition. We also thank the Editor, the Associate Editor, the Editor's Assistant, and two anonymous reviewers that helped to improve the final version of the paper.

References

- Archie, G. E. (1942). The electrical resistivity log as an aid in determining some reservoir characteristics. *Transactions of the AIME*, 146(01), 54–62. <https://doi.org/10.2118/942054-G>
- Arp, C., & Cherry, J. (2020). Seasonal maximum ice thickness data for rivers and lakes in Alaska from 1962 to 2019. <https://doi.org/10.18739/A26688J9Z>
- Arp, C. D., Drew, K. A., & Bondurant, A. C. (2023). Observation of a rapid lake-drainage event in the Arctic: Set-up and trigger mechanisms, outburst flood behaviour, and broader fluvial impacts. *Earth Surface Processes and Landforms*, 48(8), 1615–1629. <https://doi.org/10.1002/esp.5571>
- Arp, C. D., Jones, B. M., Grosse, G., Bondurant, A. C., Romanovsky, V. E., Hinkel, K. M., & Parsekian, A. D. (2016). Threshold sensitivity of shallow Arctic lakes and sublake permafrost to changing winter climate. *Geophysical Research Letters*, 43(12), 6358–6365. <https://doi.org/10.1002/2016gl068506>
- Arp, C. D., Jones, B. M., Lu, Z., & Whitman, M. S. (2012). Shifting balance of thermokarst lake ice regimes across the Arctic Coastal Plain of northern Alaska. *Geophysical Research Letters*, 39(16), L16503. <https://doi.org/10.1029/2012gl052518>
- Arp, C. D., Jones, B. M., Urban, F. E., & Grosse, G. (2011). Hydrogeomorphic processes of thermokarst lakes with grounded-ice and floating-ice regimes on the Arctic coastal plain, Alaska. *Hydrological Processes*, 25(15), 2422–2438. <https://doi.org/10.1002/hyp.8019>
- Bartsch, A., Pointner, G., Leibman, M. O., Dvornikov, Y. A., Khomutov, A. V., & Trofaier, A. M. (2017). Circumpolar mapping of ground-fast lake ice. *Frontiers in Earth Science*, 5. <https://doi.org/10.3389/feart.2017.00012>

Biggar, K. W., & Sego, D. C. (1993). Field pile load tests in saline permafrost. II. Analysis of results. *Canadian Geotechnical Journal*, 30(1), 46–59. <https://doi.org/10.1139/t93-005>

Biskaborn, B. K., Smith, S. L., Noetzli, J., Matthes, H., Vieira, G., Streletschi, D. A., et al. (2019). Permafrost is warming at a global scale. *Nature Communications*, 10(1), 264. <https://doi.org/10.1038/s41467-018-08240-4>

Brigham-Grette, J., & Hopkins, D. M. (1995). Emergent marine record and paleoclimate of the last interglaciation along the Northwest Alaskan Coast. *Quaternary Research*, 43(2), 159–173. <https://doi.org/10.1006/qres.1995.1017>

Bristol, E. M., Connolly, C. T., Lorenson, T. D., Richmond, B. M., Ilgen, A. G., Choens, R. C., et al. (2021). Geochemistry of coastal permafrost and erosion-driven organic matter fluxes to the Beaufort Sea near Drew Point, Alaska. *Frontiers in Earth Science*, 8, 639. <https://doi.org/10.3389/feart.2020.598933>

Brouchkov, A. (2002). Nature and distribution of frozen saline sediments on the Russian Arctic coast. *Permafrost and Periglacial Processes*, 13(2), 83–90. <https://doi.org/10.1002/ppp.411>

Brouchkov, A. (2003). Frozen saline soils of the Arctic coast: Their distribution and engineering properties. In M. Phillips, S. M. Springman, & L. U. Arenson (Eds.), *Proceedings of the eighth international conference on permafrost, Zurich, Switzerland* (Vol. 7, pp. 95–100).

Brown, J. (1969). *Ionic concentration gradients in permafrost, Barrow, Alaska*. US Army Cold Regions Research and Engineering Laboratory, CRREL Research Report 272 (26 pp.).

Creighton, A. L., Parsekian, A. D., Angelopoulos, M., Jones, B. M., Bondurant, A., Engram, M., et al. (2018). Transient electromagnetic surveys for the determination of Talik depth and geometry beneath Thermokarst lakes. *Journal of Geophysical Research: Solid Earth*, 123(11), 9310–9323. <https://doi.org/10.1029/2018JB016121>

Dafflon, B., Hubbard, S., Ulrich, C., Peterson, J., Wu, Y., Wainwright, H., & Kneafsey, T. J. (2016). Geophysical estimation of shallow permafrost distribution and properties in an ice-wedge polygon-dominated Arctic tundra region. *Geophysics*, 81(1), WA247–WA263. <https://doi.org/10.1190/GEO2015-0175.1>

Dammann, D. O., Eriksson, L. E. B., Mahoney, A. R., Stevens, C. W., Van der Sanden, J., Eicken, H., et al. (2018). Mapping Arctic Bottomfast Sea Ice using SAR interferometry. *Remote Sensing*, 10(5), 720. <https://doi.org/10.3390/rs10050720>

Daniels, J. J., Keller, G. V., & Jacobson, J. J. (1976). Computer-assisted interpretation of electromagnetic soundings over a permafrost section. *Geophysics*, 41(4), 752–765. <https://doi.org/10.1190/1.1440647>

Engram, M., Arp, C. D., Jones, B. M., Ajadi, O. A., & Meyer, F. J. (2018). Analyzing floating and bedfast lake ice regimes across Arctic Alaska using 25 years of space-borne SAR imagery. *Remote Sensing of Environment*, 209, 660–676. <https://doi.org/10.1016/j.rse.2018.02.022>

Gilichinsky, D., Rivkina, E., Scherbakova, V., Laurinavichius, K., & Tiedje, J. (2003). Supercooled water brines within permafrost—An unknown ecological niche for microorganisms: A model for astrobiology. *Astrobiology*, 3(2), 331–341. <https://doi.org/10.1089/153110703769016424>

Grosse, G., Jones, B., & Arp, C. (2013). 8.21 Thermokarst lakes, drainage, and drained basins. In J. F. Shroder (Ed.), *Treatise on geomorphology* (pp. 325–353). Academic Press. <https://doi.org/10.1016/B978-0-12-374739-6.00216-5>

Grunblatt, J., & Atwood, D. (2014). Mapping lakes for winter liquid water availability using SAR on the North Slope of Alaska. *International Journal of Applied Earth Observation and Geoinformation*, 27, 63–69. <https://doi.org/10.1016/j.jag.2013.05.006>

Hauck, C. (2002). Frozen ground monitoring using DC resistivity tomography. *Geophysical Research Letters*, 29(21), 12–21. <https://doi.org/10.1029/2002gl014995>

Hauck, C., & Mühl, D. V. (2003). Inversion and interpretation of two-dimensional geoelectrical measurements for detecting permafrost in mountainous regions. *Permafrost and Periglacial Processes*, 14(4), 305–318. <https://doi.org/10.1002/ppp.462>

Hilbich, C., Hauck, C., Hoelzle, M., Scherler, M., Schudel, L., Völksch, I., et al. (2008). Monitoring mountain permafrost evolution using electrical resistivity tomography: A 7-year study of seasonal, annual, and long-term variations at Schilthorn, Swiss Alps. *Journal of Geophysical Research*, 113(F1), F01S90. <https://doi.org/10.1029/2007jf000799>

Himmelstoss, E. A., Henderson, R. E., Kratzmann, M. G., & Farris, A. S. (2021). Digital shoreline analysis system (DSAS) version 5.1 user guide (No. 2021-1091). Open-file report. *U.S. Geological Survey*. <https://doi.org/10.3133/ofr20211091>

Hinkel, K. M., Paetzold, F., Nelson, F. E., & Bockheim, J. G. (2001). Patterns of soil temperature and moisture in the active layer and upper permafrost at Barrow, Alaska: 1993–1999. *Global and Planetary Change*, 29(3–4), 293–309. [https://doi.org/10.1016/s0921-8181\(01\)00096-0](https://doi.org/10.1016/s0921-8181(01)00096-0)

Hivon, E. G., & Sego, D. C. (1993). Distribution of saline permafrost in the Northwest Territories, Canada. *Canadian Geotechnical Journal*, 30(3), 506–514. <https://doi.org/10.1139/t93-043>

Iwahana, G., Cooper, Z. S., Carpenter, S. D., Deming, J. W., & Eicken, H. (2021). Intra-ice and intra-sediment cryopeg brine occurrence in permafrost near Utqiagvik (Barrow). *Permafrost and Periglacial Processes*, 32(3), 427–446. <https://doi.org/10.1002/ppp.2101>

Jones, B., Kanevskiy, M., Parsekian, A., Bergstedt, H., Jones, M. W., Rangel, R., et al. (2023a). Saline permafrost degradation below a shallow thermokarst lake in northern Alaska, 2008–2023 [Dataset]. Arctic Data Center. <https://doi.org/10.18739/A20POWS3K>

Jones, B. M., & Arp, C. D. (2015). Observing a catastrophic thermokarst lake drainage in northern Alaska. *Permafrost and Periglacial Processes*, 26(2), 119–128. <https://doi.org/10.1002/ppp.1842>

Jones, B. M., Arp, C. D., Grosse, G., Nitze, I., Lara, M. J., Whitman, M. S., et al. (2020). Identifying historical and future potential lake drainage events on the western Arctic coastal plain of Alaska. *Permafrost and Periglacial Processes*, 31(1), 110–127. <https://doi.org/10.1002/ppp.2038>

Jones, B. M., Farquharson, L. M., Baughman, C. A., Buzard, R. M., Arp, C. D., Grosse, G., et al. (2018). A decade of remotely sensed observations highlight complex processes linked to coastal permafrost bluff erosion in the Arctic. *Environmental Research Letters*, 13(11), 115001. <https://doi.org/10.1088/1748-9326/aae471>

Jones, B. M., Grosse, G., Farquharson, L. M., Roy-Léveillé, P., Veremeeva, A., Kanevskiy, M. Z., et al. (2022). Lake and drained lake basin systems in lowland permafrost regions. *Nature Reviews Earth & Environment*, 3(1), 85–98. <https://doi.org/10.1038/s43017-021-00238-9>

Jones, B. M., Schaeffer Tessier, S., Tessier, T., Brubaker, M., Brook, M., Schaeffer, J., et al. (2023b). Integrating local environmental observations and remote sensing to better understand the life cycle of a thermokarst lake in Arctic Alaska. *Arctic Antarctic and Alpine Research*, 55(1), 2195518. <https://doi.org/10.1080/15230430.2023.2195518>

Jorgenson, M. T., & Shur, Y. (2007). Evolution of lakes and basins in northern Alaska and discussion of the thaw lake cycle. *Journal of Geophysical Research*, 112(F2), F02S17. <https://doi.org/10.1029/2006JF000531>

Kanevskiy, M., Shur, Y., Jorgenson, M. T., Ping, C.-L., Michaelson, G. J., Fortier, D., et al. (2013). Ground ice in the upper permafrost of the Beaufort Sea coast of Alaska. *Cold Regions Science and Technology*, 85, 56–70. <https://doi.org/10.1016/j.coldregions.2012.08.002>

Lantz, T. C., Zhang, Y., & Kokelj, S. V. (2022). Impacts of ecological succession and climate warming on permafrost aggradation in drained lake basins of the Tuktoyaktuk Coastlands, Northwest Territories, Canada. *Permafrost and Periglacial Processes*, 33(2), 176–192. <https://doi.org/10.1002/ppp.2143>

Lorenson, T. D., Oberle, F. J., Johnson, C. D., Richmond, B. M., Erikson, L. H., Gibbs, A., et al. (2018). Cryopegs of Northern Alaska 2018 (pp. B31H–2587).

Miller, D. L., & Johnson, L. A. (1990). Pile settlement in saline permafrost: A case history. In *Proceedings of the 5th Canadian permafrost conference, Quebec* (pp. 371–378).

Murfitt, J., & Duguay, C. R. (2021). 50 years of lake ice research from active microwave remote sensing: Progress and prospects. *Remote Sensing of Environment*, 264, 112616. <https://doi.org/10.1016/j.rse.2021.112616>

Muster, S., Riley, W. J., Roth, K., Langer, M., Cresto Aleina, F., Koven, C. D., et al. (2019). Size Distributions of arctic waterbodies reveal consistent relations in their statistical moments in space and time. *Frontiers in Earth Science*, 7. <https://doi.org/10.3389/feart.2019.00005>

Nersesova, Z. A., & Poire, I. V. (1952). *Concerning the melting of ice in the ground at negative temperatures* (No. 52–114). Open-File Report. s.n. <https://doi.org/10.3133/ofr52114>

O'Sullivan, J. B. (1966). Geochemistry of permafrost, Barrow, Alaska. In *Permafrost international conference* (pp. 30–37). National Academy of Sciences Lafayette.

Parsekian, A., Creighton, A., Jones, B., Bondurant, A., & Arp, C. (2018). Arctic lake transient electromagnetic (TEM) soundings 2016–2017 [Dataset]. Arctic Data Center. <https://doi.org/10.18739/A21N7XN1V>

Parsekian, A. D., Creighton, A. L., Jones, B. M., & Arp, C. D. (2019). Surface nuclear magnetic resonance observations of permafrost thaw below floating, bedfast, and transitional ice lakes. *Geophysics*, 84(3), EN33–EN45. <https://doi.org/10.1190/geo2018-0563.1>

Pointner, G., Bartsch, A., Forbes, B. C., & Kumpula, T. (2019). The role of lake size and local phenomena for monitoring ground-fast lake ice. *International Journal of Remote Sensing*, 40(3), 832–858. <https://doi.org/10.1080/01431161.2018.1519281>

Rangel, R. C., Parsekian, A. D., Farquharson, L. M., Jones, B. M., Ohara, N., Creighton, A. L., et al. (2021). Geophysical observations of taliks below drained lake basins on the Arctic Coastal Plain of Alaska. *Journal of Geophysical Research: Solid Earth*, 126(3), e2020JB020889. <https://doi.org/10.1029/2020JB020889>

Roy-Leveillee, P., & Burn, C. R. (2017). Near-shore talik development beneath shallow water in expanding thermokarst lakes, Old Crow Flats, Yukon. *Journal of Geophysical Research: Earth Surface*, 122(5), 1070–1089. <https://doi.org/10.1002/2016JF004022>

Shur, Y., Jones, B. M., Kanavskiy, M., Jorgenson, T., Jones, M. K. W., Fortier, D., et al. (2021). Fluvio-thermal erosion and thermal denudation in the yedoma region of northern Alaska: Revisiting the Itkillik River exposure. *Permafrost and Periglacial Processes*, 32(2), 277–298. <https://doi.org/10.1002/ppp.2105>

Wan, X., Lai, Y., & Wang, C. (2015). Experimental study on the freezing temperatures of saline silty soils. *Permafrost and Periglacial Processes*, 26(2), 175–187. <https://doi.org/10.1002/ppp.1837>

Weeks, W. F., Fountain, A. G., Bryan, M. L., & Elachi, C. (1978). Differences in radar return from ice-covered North Slope Lakes. *Journal of Geophysical Research*, 83(C8), 4069–4073. <https://doi.org/10.1029/JC083iC08p04069>

Widhalm, B., Bartsch, A., & Goler, R. (2018). Simplified normalization of C-band synthetic aperture radar data for terrestrial applications in high latitude environments. *Remote Sensing*, 10(4), 551. <https://doi.org/10.3390/rs10040551>

Wolfe, S., Murton, J., Bateman, M., & Barlow, J. (2020). Oriented-lake development in the context of late Quaternary landscape evolution, McKinley Bay Coastal Plain, western Arctic Canada. *Quaternary Science Reviews*, 242, 106414. <https://doi.org/10.1016/j.quascirev.2020.106414>